Nonlinear effects in ultrasmall Silicon-On-Insulator ring resonators

Gino Priem, Pieter Dumon, Wim Bogaerts, Dries Van Thourhout,
Geert Morthier, and Roel Baets

Photonics Research Group, Dept. of Information Technology,
Ghent University - IMEC, Belgium

ABSTRACT

We investigate the significance of secondary effects caused by free carrier accumulation and subsequent heating on the nonlinear behaviour of ultrasmall Silicon-On-Insulator ring resonators. All-optical bistability based on thermal dispersion was experimentally obtained for an input power of only 0.28 mW. At higher powers, pulsating behaviour was observed which is problematic for the stability of thermal memory and switching operations. Using free carrier dispersion, we also demonstrate all-optical wavelength conversion with a pulse length of 10 ns, indicating that bitrates of 0.1 Gb/s are feasible. Also here, the presence of unstable pulsations was observed, leading to significant errors in the converted data pattern.

Keywords: two-photon absorption, free-carrier dispersion, optical bistability, optical instability, photonic wires, ring resonators, Silicon-on-Insulator

1. INTRODUCTION

Today, optical fiber forms the basis for the modern long-haul telecom infrastructure and is already starting to penetrate the markets of high-end local area networks and short distance applications. To fully utilize its potential, improved switching and processing functionalities are however necessary inside the optical layer. Although low-cost integration while maintaining optical-electrical conversions is a first step, all-optical signal processing is expected to form the real breakthrough towards ultra-high bandwidth telecommunication. In the context of the recent advances in fabricating high-quality nanophotonic devices, ultrafast nonlinear optics forms an excellent candidate to achieve this goal.

In standard semiconductor materials, ultrafast nonlinear effects like the optical Kerr effect and two-photon absorption (2PA) are typically very small, leading to the requirement of high input powers or long devices for practical applications. Photonic wire structures fabricated in high contrast systems such as Silicon-on-Insulator (SOI) however allow strong transverse confinement of the light within submicron dimensions, so that the nonlinear interaction is significantly enhanced. Using these structures, ultrafast nonlinear wavelength conversion has already been demonstrated for pulse trains at 40 GHz.[1,2] This optical confinement can even be further improved by using optical resonators. Inside these resonators, the field is enhanced and the pulse is slowed down, so that the nonlinear response is even larger, however at the cost of a reduction in bandwidth.[3,4]

A significant problem for ultrafast nonlinear signal processing is however the presence of secondary phenomena like carrier generation and heating.[5,6] As these effects are not only much slower, but also much larger, they can easily dominate the nonlinear response of the device[6–8] and lead to instabilities.[6,9] On the other hand, they can also be used for all-optical signal processing, but at much lower data rates. These different aspects are investigated in this work.

Further author information:
Send correspondence concerning nonlinear work to Gino Priem; E-mail: Gino.Priem@intec.UGent.be
Send correspondence concerning fabrication to Pieter Dumon; E-mail: Pieter.Dumon@intec.UGent.be

Integrated Optics, Silicon Photonics, and Photonic Integrated Circuits, edited by Giancarlo C. Righini,
Proc. of SPIE Vol. 6183, 61831A, (2006) · 0277-786X/06/$15 · doi: 10.1117/12.668249

Nonlinear effects in ultrasmall Silicon-On-Insulator ring resonators

Gino Priem, Pieter Dumon, Wim Bogaerts, Dries Van Thourhout,
Geert Morthier, and Roel Baets

Photonics Research Group, Dept. of Information Technology,
Ghent University - IMEC, Belgium

ABSTRACT

We investigate the significance of secondary effects caused by free carrier accumulation and subsequent heating on the nonlinear behaviour of ultrasmall Silicon-On-Insulator ring resonators. All-optical bistability based on thermal dispersion was experimentally obtained for an input power of only 0.28 mW. At higher powers, pulsating behaviour was observed which is problematic for the stability of thermal memory and switching operations. Using free carrier dispersion, we also demonstrate all-optical wavelength conversion with a pulse length of 10 ns, indicating that bitrates of 0.1 Gb/s are feasible. Also here, the presence of unstable pulsations was observed, leading to significant errors in the converted data pattern.

Keywords: two-photon absorption, free-carrier dispersion, optical bistability, optical instability, photonic wires, ring resonators, Silicon-on-Insulator

1. INTRODUCTION

Today, optical fiber forms the basis for the modern long-haul telecom infrastructure and is already starting to penetrate the markets of high-end local area networks and short distance applications. To fully utilize its potential, improved switching and processing functionalities are however necessary inside the optical layer. Although low-cost integration while maintaining optical-electrical conversions is a first step, all-optical signal processing is expected to form the real breakthrough towards ultra-high bandwidth telecommunication. In the context of the recent advances in fabricating high-quality nanophotonic devices, ultrafast nonlinear optics forms an excellent candidate to achieve this goal.

In standard semiconductor materials, ultrafast nonlinear effects like the optical Kerr effect and two-photon absorption (2PA) are typically very small, leading to the requirement of high input powers or long devices for practical applications. Photonic wire structures fabricated in high contrast systems such as Silicon-on-Insulator (SOI) however allow strong transverse confinement of the light within submicron dimensions, so that the nonlinear interaction is significantly enhanced. Using these structures, ultrafast nonlinear wavelength conversion has already been demonstrated for pulse trains at 40 GHz.[1,2] This optical confinement can even be further improved by using optical resonators. Inside these resonators, the field is enhanced and the pulse is slowed down, so that the nonlinear response is even larger, however at the cost of a reduction in bandwidth.[3,4]

A significant problem for ultrafast nonlinear signal processing is however the presence of secondary phenomena like carrier generation and heating.[5,6] As these effects are not only much slower, but also much larger, they can easily dominate the nonlinear response of the device[6–8] and lead to instabilities.[6,9] On the other hand, they can also be used for all-optical signal processing, but at much lower data rates. These different aspects are investigated in this work.

Further author information:
Send correspondence concerning nonlinear work to Gino Priem; E-mail: Gino.Priem@intec.UGent.be
Send correspondence concerning fabrication to Pieter Dumon; E-mail: Pieter.Dumon@intec.UGent.be

Integrated Optics, Silicon Photonics, and Photonic Integrated Circuits, edited by Giancarlo C. Righini,
Proc. of SPIE Vol. 6183, 61831A, (2006) · 0277-786X/06/$15 · doi: 10.1117/12.668249

2. NONLINEAR INTERACTION PICTURE OF A SILICON SYSTEM

At the telecom wavelength of 1550 nm, light is absorbed in the Silicon material by means of two-photon absorption, which is the counterpart of the intensity dependent refractive index effect known as the optical Kerr effect. Through this absorption process, free carriers are excited in the material, which give rise to additional absorption (Free Carrier Absorption, FCA) and also a change in refractive index (Free Carrier Dispersion, FCD).

After a while, these carriers will recombine and in the case of submicron structures (such as photonic wires), this is mainly due to surface recombination. This interband relaxation process together with the intraband relaxation effects from carriers created due to 2PA and excited by FCA will mainly lead to phonon creation, which results in heating of the structure and gives rise to a thermal refractive index change. Due to conduction and convection, the structure finally cools down to a steady-state temperature.

This whole process is summarized in Fig. 1.

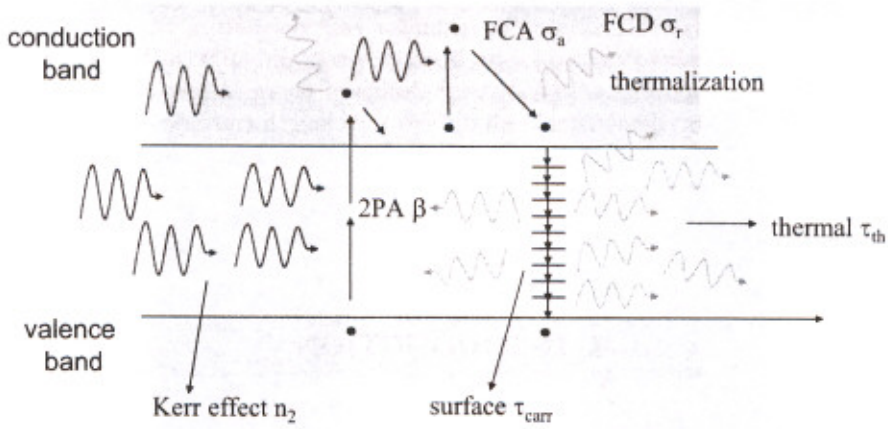

Figure 1. Competing nonlinear effects in the Silicon material system for wavelengths above half the band gap.

3. FABRICATED STRUCTURES

For our nonlinear measurements, ring resonator structures were designed on a SOI wafer with a thickness of the Silicon layer of 220 nm and a burried oxide of 1 μm. By means of a deep UV lithography stepper with a 248 nm illumination wavelength, the patterns are defined in the resist, after which a dry etching process is used to transfers them into the Silicon layer. A detailed overview of the processing steps can be found in Ref. 10. The processes are intrinsically CMOS processes, which are characterized and adapted for the fabrication of photonic devices. An example of such a ring resonator structure is shown in Fig. 2.

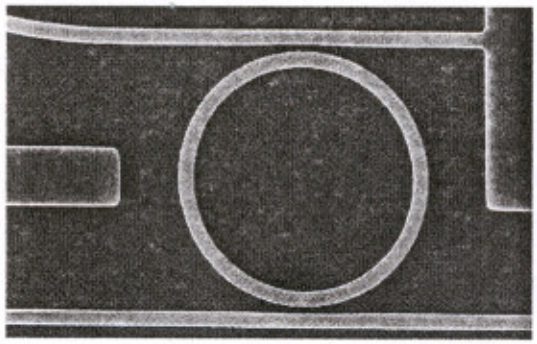

Figure 2. Example of a ring resonator structure fabricated through deep UV lithography.

Acceptable linear losses were obtained for ring radii down to 3 μm. For our experiments, we used a ring resonator with a radius of 4 μm and wire width of approximately 540 nm.

4. LOW-POWER MEASUREMENTS

Low-power measurements were performed to determine the free spectral range and the resonance bandwidth. The resulting transmission spectrum of the pass port and the drop port is plotted in Fig. 3.

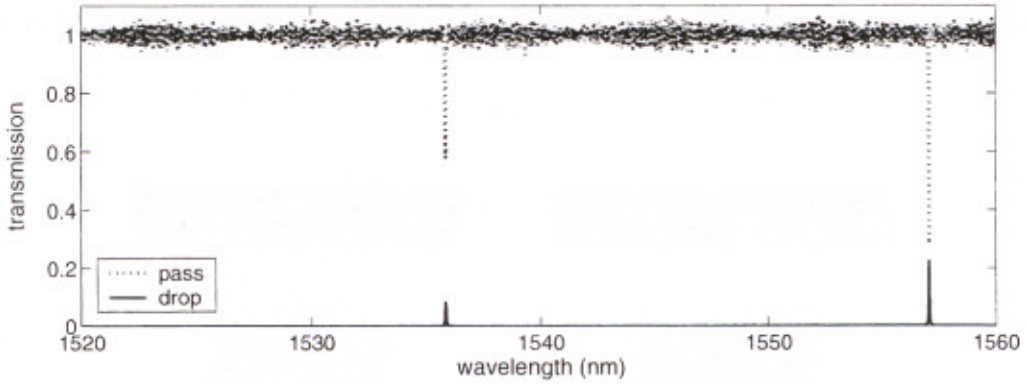

Figure 3. Normalized transmission of the pass and the drop port in the low-power regime.

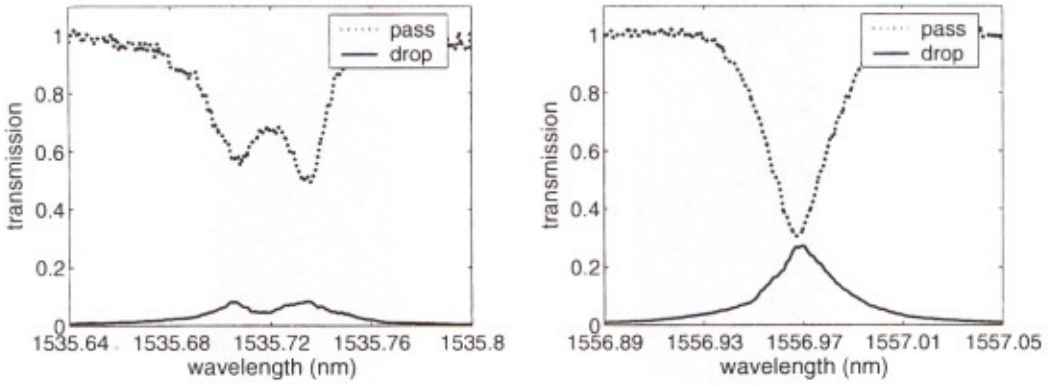

Figure 4. (left) Detail around the resonance wavelength 1535.72 nm. (right) Detail around the resonance wavelength 1556.97 nm.

The resonance at the wavelength 1535.72 nm has a bandwidth of 81 pm corresponding to a Q-factor of 19000. The bandwidth of the resonance at the wavelength 1556.97 nm is approximately 56 pm, leading to a Q-factor of 28000. The measured free spectral range is 21.25 nm. The peak transmission at the resonances is respectively 0.08 and 0.27 (Fig. 4). As can be seen, the resonance at the wavelength 1535.72 nm is slightly split due to surface roughness induced backscattering.

5. HIGH-POWER MEASUREMENTS

Continuous-wave experiments

To determine the impact of secondary effects on the resonator behaviour, continuous-wave measurements were performed first. The signal power was varied from 0.069 mW in steps of 3dB and from 0.277 mW on in steps of 1.5dB. The resulting drop transmission spectra are shown in Fig. 5. Due to the fact that the laser source could

Acceptable linear losses were obtained for ring radii down to 3 μm. For our experiments, we used a ring resonator with a radius of 4 μm and wire width of approximately 540 nm.

4. LOW-POWER MEASUREMENTS

Low-power measurements were performed to determine the free spectral range and the resonance bandwidth. The resulting transmission spectrum of the pass port and the drop port is plotted in Fig. 3.

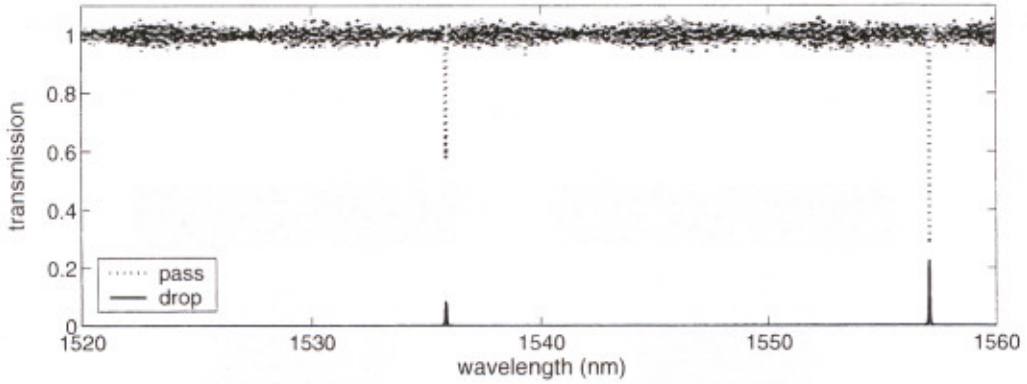

Figure 3. Normalized transmission of the pass and the drop port in the low-power regime.

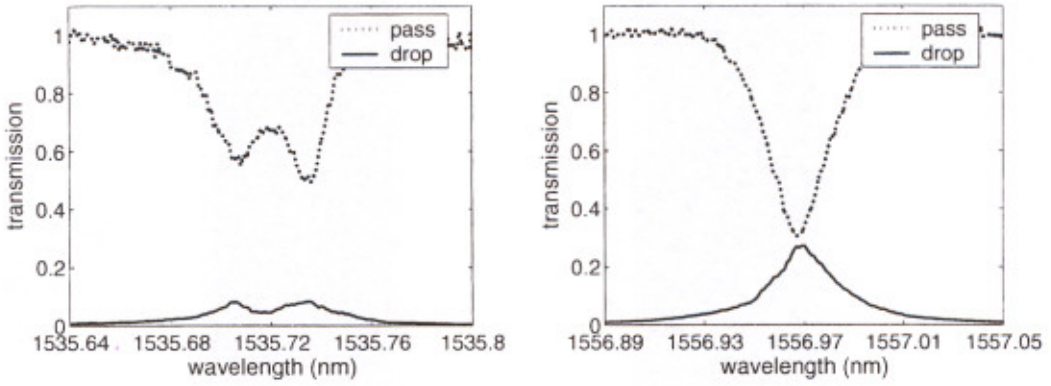

Figure 4. (left) Detail around the resonance wavelength 1535.72 nm. (right) Detail around the resonance wavelength 1556.97 nm.

The resonance at the wavelength 1535.72 nm has a bandwidth of 81 pm corresponding to a Q-factor of 19000. The bandwidth of the resonance at the wavelength 1556.97 nm is approximately 56 pm, leading to a Q-factor of 28000. The measured free spectral range is 21.25 nm. The peak transmission at the resonances is respectively 0.08 and 0.27 (Fig. 4). As can be seen, the resonance at the wavelength 1535.72 nm is slightly split due to surface roughness induced backscattering.

5. HIGH-POWER MEASUREMENTS

Continuous-wave experiments

To determine the impact of secondary effects on the resonator behaviour, continuous-wave measurements were performed first. The signal power was varied from 0.069 mW in steps of 3dB and from 0.277 mW on in steps of 1.5dB. The resulting drop transmission spectra are shown in Fig. 5. Due to the fact that the laser source could

only be swept in the upward wavelength direction, only the upper (bistable) arm is plotted. From the steep declines in the transmission, it can however be seen that all-optical bistability is obtained for powers of 0.277 mW and above. This value is the lowest reported value for ring resonator structures as we know,[10] but higher than the best results obtained with PhC nanocavities.[7,11,12] The latter however are standing-wave resonators, which have the benefit of better nonlinear interaction due to the presence of a contrapropagating wave inside the cavity (3×, 10× and 35× higher for respectively third-, fifth- and seventh-order nonlinear effect[13]).

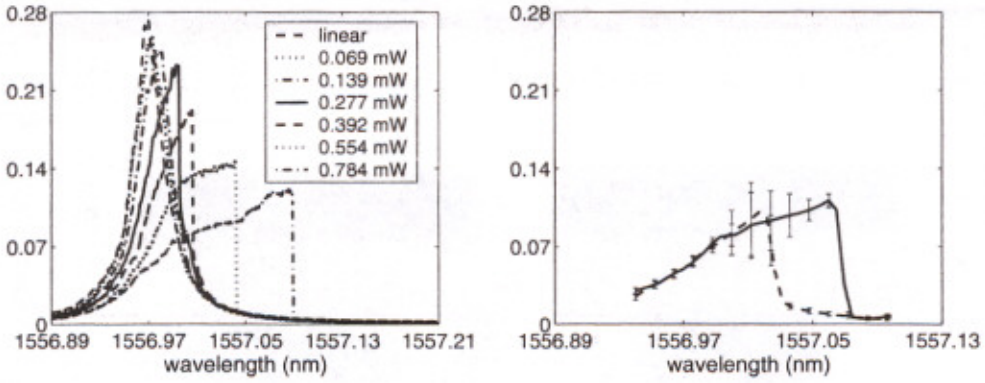

Figure 5. (left) Normalized transmission of the drop port in the high-power regime. (right) Average drop transmission spectrum together with the standard deviation for an input power of 0.76 mW. Both (bistable) arms are plotted as the sweep was carried out manually.

From the reduction of the transmission due to 2PA and FCA, information concerning the carrier lifetime can be derived. The shift of the resonance frequency, which is caused by the Kerr effect, FCD and thermal dispersion, on the other hand provides information about the thermal lifetime. This was done in Ref. 6: a carrier-dependent carrier lifetime of the order of $1 - 10$ ns was derived for carrier densities in the range of $10^{16} - 10^{17}\,\mathrm{cm}^{-3}$ and a thermal lifetime of 65 ns was obtained. The different contributions to the refractive index change are plotted in Fig. 6. A linear thermal contribution is present in addition to the terms discussed in Section 2 due to surface state absorption (SSA).

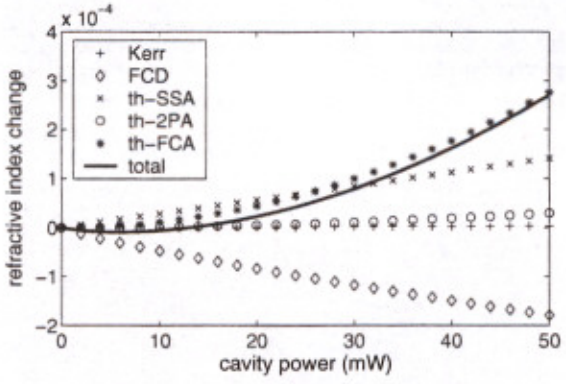

Figure 6. Different contributions to the refractive index change as function of power: Kerr effect n_2, free-carrier dispersion (FCD), thermal dispersion due to surface-state absorption (th-SSA), thermal dispersion due to two-photon absorption (th-2PA), thermal dispersion due to free-carrier absorption (th-FCA)

As can be seen, thermal contributions due to FCA and SSA are dominant, which could already be concluded from the bistability on the upper wavelength side. However, also the FCD refractive index change is quite large.

The presence of two large opposite refractive index effects with different time constants can lead to a periodic pulsating output signal, when the resonator is excited by a CW pump beam. Qualitatively, this behaviour can be understood as a circling around the bistability loop.[14,15] This was observed indirectly by measuring the standard deviation of the output signal, as shown in Fig. 5, for an input power of 0.76 mW. Both (bistable) arms are now present as the sweep was carried out manually.

Due to the presence of noise in the input signal, the obtained oscillations were however pseudo-periodic, so that the periodicity could not be visualized on the oscilloscope. However two clearly distinct power levels were obtained. This is for instance shown for 1557.02 nm in Fig. 7, while the results at 1557.03 nm (lower arm) only has a single power level.

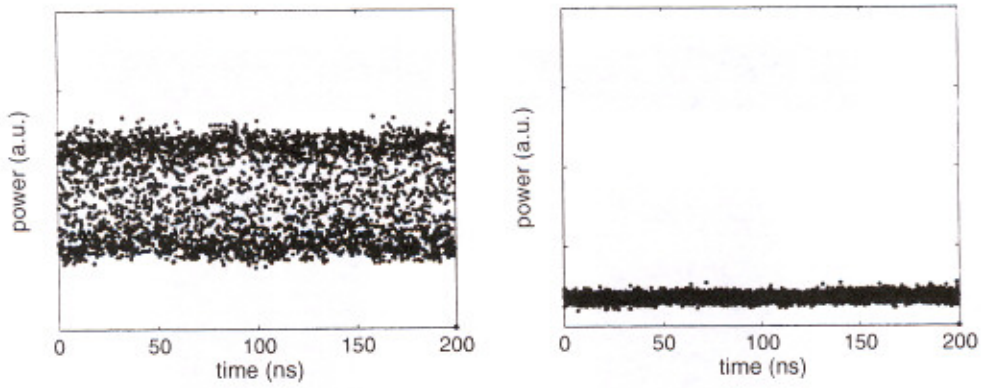

Figure 7. Oscilloscope data at the wavelength 1557.02 nm (left) and 1557.03 nm (right) for an input power of 0.76 mW. In the first plot, two different power levels can clearly be distinguished.

Pump-probe experiments

From the analysis above, it is clear that secondary effects will dominate the nonlinear behaviour in the case of standard Non-Return-to-Zero (NRZ) data streams, making it impossible to use ultrafast nonlinear phenomena like the Kerr effect and two-photon absorption. A solution would be to go to lower repetition rates and thus adjusted data formats.[1,2] Alternatively, one could use these secondary effects themselves within the limitation of their lifetime and use the advantage of much lower operating powers. Applications along the lines of all-optical packet routing are however possible. As the carrier effects we observed had a recovery time up to 10 ns, a bitrate of only 0.1 Gb/s was used.

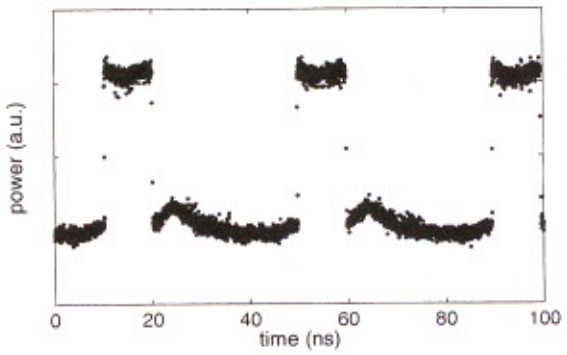

Figure 8. Pump signal inserted on the resonance at 1556.97 nm.

The presence of two large opposite refractive index effects with different time constants can lead to a periodic pulsating output signal, when the resonator is excited by a CW pump beam. Qualitatively, this behaviour can be understood as a circling around the bistability loop.[14,15] This was observed indirectly by measuring the standard deviation of the output signal, as shown in Fig. 5, for an input power of 0.76 mW. Both (bistable) arms are now present as the sweep was carried out manually.

Due to the presence of noise in the input signal, the obtained oscillations were however pseudo-periodic, so that the periodicity could not be visualized on the oscilloscope. However two clearly distinct power levels were obtained. This is for instance shown for 1557.02 nm in Fig. 7, while the results at 1557.03 nm (lower arm) only has a single power level.

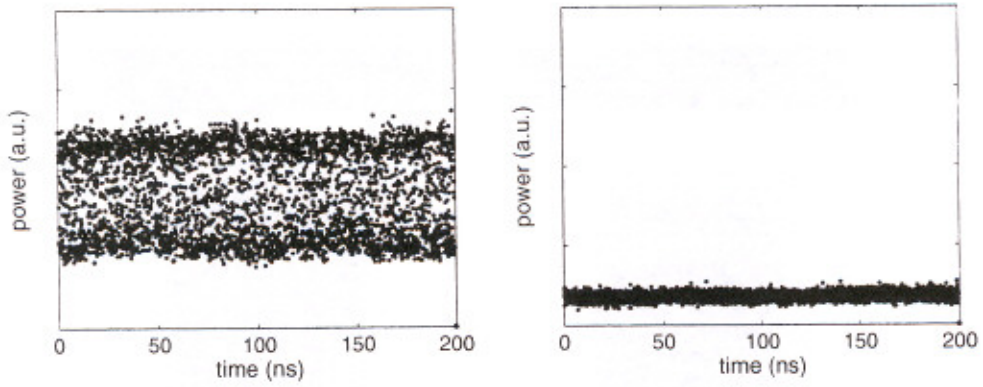

Figure 7. Oscilloscope data at the wavelength 1557.02 nm (left) and 1557.03 nm (right) for an input power of 0.76 mW. In the first plot, two different power levels can clearly be distinguished.

Pump-probe experiments

From the analysis above, it is clear that secondary effects will dominate the nonlinear behaviour in the case of standard Non-Return-to-Zero (NRZ) data streams, making it impossible to use ultrafast nonlinear phenomena like the Kerr effect and two-photon absorption. A solution would be to go to lower repetition rates and thus adjusted data formats.[1,2] Alternatively, one could use these secondary effects themselves within the limitation of their lifetime and use the advantage of much lower operating powers. Applications along the lines of all-optical packet routing are however possible. As the carrier effects we observed had a recovery time up to 10 ns, a bitrate of only 0.1 Gb/s was used.

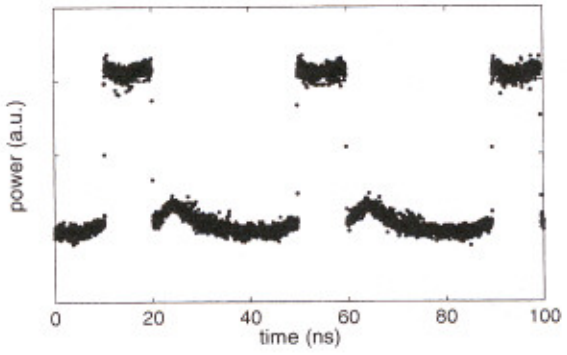

Figure 8. Pump signal inserted on the resonance at 1556.97 nm.

To demonstrate this behaviour, a pump signal with a peak power of 0.66 mW and an extinction ratio of 5 dB was inserted on the second resonance, while a CW probe signal was positioned near the first resonance wavelength 1535.72 nm. Depending on the probe wavelength offset, either non-inverted or inverted wavelength conversion is expected. To observe this clearly, a 10001000... bit pattern was used (Fig. 8). The obtained output probe signals are plotted in Fig. 9. As expected, a bit pattern of either 10001000... or 01110111... is obtained. We measured an extinction ratio of respectively 2.7 dB and 3.8 dB. The bitrate is clearly limited by the carrier lifetime. While the rise time is typically fast, the recovery time is of the order of 10 ns in agreement with our theoretical results. The thermal background was estimated at $\Delta T = 0.85\,\mathrm{K}$.

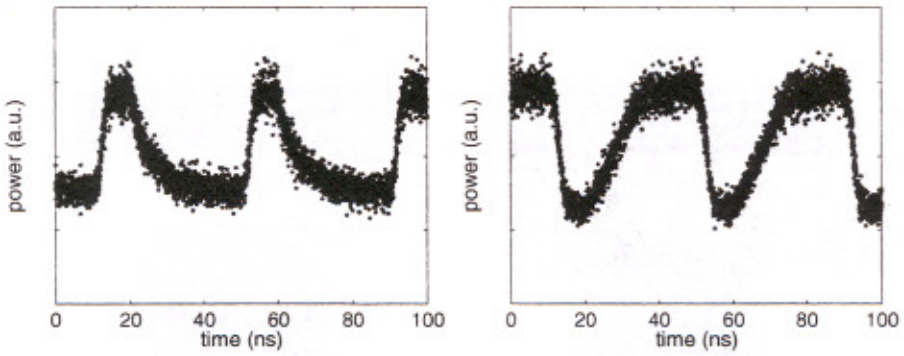

Figure 9. (left) Measured output probe signals at the wavelengths 1535.72 nm (left) and 1535.80 nm (right) for a pump power of 0.66 mW.

Higher contrasts are expected by optimizing the position of both the pump and the probe signals. Another approach would be using higher powers, however as in the continuous-wave experiments, interaction between the free-carrier and the thermal effects can lead to errors in the converted bit pattern. This is shown in Fig. 10 for the same setup with an input power of 1.32 mW.

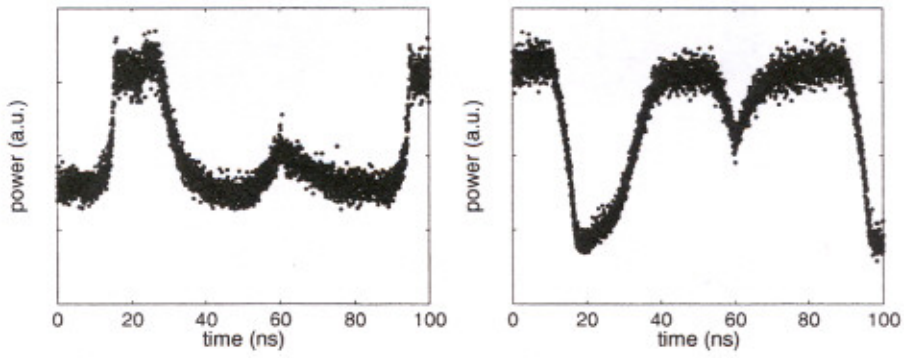

Figure 10. (left) Measured output probe signals at the wavelengths 1535.72 nm (left) and 1535.80 nm (right) for a pump power of 1.32 mW.

6. CONCLUSIONS

We discussed and demonstrated the impact of secondary effects on the nonlinear behaviour of Silicon-on-Insulator ring resonators. It was shown that this behaviour is dominated by thermal dispersion, but also a significant

contribution due to free carriers is present. The lifetime of these thermal and free-carrier effects were respectively estimated at 65 ns and 1-10 ns. All-optical bistability was obtained with input powers of only 0.28 mW. We also observed quasi-periodic pulsating behaviour for higher input powers due to an interaction between the two dominant refractive effects. which have a different sign and a different time constant.

Limited by the carrier lifetime, we demonstrated both non-inverted and inverted all-optical wavelength conversion induced by free-carrier dispersion at a bitrate of 0.1 Gb/s. Despite this low bitrate, applications in the field of all-optical packet routing could be possible. At higher pump power, again unstable behaviour was observed leading to errors in the obtained data pattern.

Both the limited bitrate and the unstable behaviour could be avoided by extracting the carriers by means of a reverse biased p-i-n structure.[16–18] We estimate that this would also allow all-optical bistability based on free-carrier dispersion.

ACKNOWLEDGMENTS

This work was supported by the EU through the Network of Excellence ePIXnet. Part of this work has been performed in the context of the Belgian IAP PHOTON Network (IAP V/18).

Gino Priem and Wim Bogaerts acknowledge the Flemish Fund for Scientific Research (FWO-Vlaanderen) for financial support. Pieter Dumon thanks the Institute for the Promotion of Innovation through Science and Technology in Flanders (IWT-Vlaanderen) for a scholarship.

REFERENCES

1. T. Liang, L. Nunes, T. Sakamoto, K. Sasagawa, T. Kawanishi, M. Tsuchiya, G. Priem, D. Van Thourhout, P. Dumon, R. Baets, and H. Tsang, "Ultrafast all-optical switching by cross-absorption modulation in Silicon wire waveguides," *Opt. Express* **13**, pp. 7298–7303, 2005.
2. L. Nunes, T. Liang, K. Abedin, T. Miyazaki, M. Tsuchiya, D. Van Thourhout, P. Dumon, R. Baets, and H. Tsang, "Low energy ultrafast switching in silicon wire waveguides," in *Proceedings of 2005 European Conference on Optical Communication (ECOC), Th4.2.3*, Glasgow, United Kingdom, 2005.
3. G. Priem, I. Notebaert, P. Bienstman, G. Morthier, and R. Baets, "Resonator-based all-optical Kerr-nonlinear phase shifting: Design and limitations," *J. Appl. Phys.* **97**, p. 023104, 2005.
4. G. Priem, I. Notebaert, B. Maes, P. Bienstman, G. Morthier, and R. Baets, "Design of all-optical nonlinear functionalities based on resonators," *IEEE J. Select. Topics Quantum Electron.* **10**, pp. 1070–1078, 2004.
5. V. Almeida, C. Barrios, R. Panepucci, and M. Lipson, "All-optical control of light on a Silicon chip," *Nature* **431**, pp. 1081–1084, 2004.
6. G. Priem, P. Dumon, W. Bogaerts, D. Van Thourhout, G. Morthier, and R. Baets, "Optical bistability and pulsating behaviour in Silicon-on-Insulator ring resonator structures," *Opt. Express* **13**, pp. 9623–9628, 2005.
7. P. Barclay, K. Srinivasan, and O. Painter, "Nonlinear response of Silicon photonic crystal microresonators excited via an integrated waveguide and fiber taper," *Opt. Express* **13**, pp. 801–820, 2005.
8. T. Liang, L. Nunes, M. Tsuchiya, K. Abedin, T. Miyazaki, D. Van Thourhout, P. Dumon, R. Baets, and H. Tsang, "Nonlinear self-distortion of picosecond optical pulses in Silicon wire waveguides," in *Proceedings of 2006 European Conference on Optical Communication (ECOC). (submitted)*, Long Beach, United States, 2006.
9. T. Johnson, "Self-induced optical modulation of the transmission through a high-q silicon microdisk resonator," *Opt. Express* **14**, pp. 817–831, 2006.
10. V. Almeida and M. Lipson, "Optical bistability on a Silicon chip," *Opt. Lett.* **29**, pp. 2387–2389, October 2004.
11. M. Notomi, A. Shinya, S. Mitsugi, G. Kira, E. Kuramochi, and T. Tanabe, "Optical bistable switching action of Si high-Q photonic-crystal nanocavities," *Opt. Express* **13**, pp. 2678–2687, 2005.

12. T. Uesugi, B.-S. Song, T. Asano, and S. Noda, "Investigation of optical nonlinearities in an ultra-high-Q Si nanocavity in a two-dimensional photonic crystal slab," *Opt. Express* **14**, pp. 377–386, 2006.
13. A. Melloni, F. Morichetti, and M. Martinelli, "Linear and nonlinear pulse propagation in coupled resonator slow-wave optical structures," *Opt. Quantum Electron.* **35**, pp. 365–379, 2003.
14. S. McCall, "Instability and regenerative pulsation phenomena in fabry-perot nonlinear optic media devices," *Appl. Phys. Lett.* **32**, pp. 284–286, 1978.
15. H. Gibbs, *Optical bistability: controlling light with light*, Academic Press. Orlando, 1th ed., 1985.
16. A. Liu, R. Jones, L. Liau, D. Samara-Rubio, D. Rubin, O. Cohen, R. Nicolaescu, and M. Paniccia, "A high-speed Silicon optical modulator based on a metal-oxide-semiconductor capacitor," *Nature* **427**, pp. 615–618, 2004.
17. S. Preble, Q. Xu, B. Schmidt, and M. Lipson, "Ultrafast all-optical modulation on a Silicon chip," *Opt. Lett.* **30**, pp. 2891–2893, 2005.
18. H. Rong, Y.-H. Kuo, A. Liu, M. Paniccia, and O. Cohen, "High efficiency wavelength conversion of 10 gb/s data in silicon waveguides," *Opt. Express* **14**, pp. 1182–1188, 2006.

PROCEEDINGS OF SPIE

Integrated Optics, Silicon Photonics, and Photonic Integrated Circuits

Giancarlo C. Righini
Chair/Editor

3–5 April 2006
Strasbourg, France

Sponsored by
SPIE Europe

Cosponsored by
Conseil General Du Bas-Rhin (France)
Communauté Urbaine de Strausbourg (France)
Région Alsace (France)
Alsace Development Agency (France)

Volume 6183

The International Society for Optical Engineering

CONF 1391

PROCEEDINGS OF SPIE

Integrated Optics, Silicon Photonics, and Photonic Integrated Circuits

Giancarlo C. Righini
Chair/Editor

3–5 April 2006
Strasbourg, France

Sponsored by
SPIE Europe

Cosponsored by
Conseil General Du Bas-Rhin (France)
Communauté Urbaine de Strasbourg (France)
Région Alsace (France)
Alsace Development Agency (France)

Cooperating Organizations
CNOP—Comité National d'Optique et de Photonique (France) • COST—Committee of Senior Officials for Scientific and Technical Research (Belgium) • EU Framework Programme (Belgium) • ESF—European Science Foundation (France) • DGaO—Deutsche Gesellschaft fuer angewandte Optik (Germany) • EOS—European Optical Society (Germany) • ePIXnet (Belgium) • FlexiDis (Netherlands) • ISIS—Infrastructures for Broadband Access in Wireless/Photonics and Integration of Strengths in Europe (France) • NEMO—Network of Excellence on Micro-Optics (Belgium) • The OLLA Project (Germany) • OPERA 2015 (Belgium) PHOREMOST (Ireland) • Photonics Cluster (United Kingdom) • RhenaPhotonics Alsace (France) • SIOF—Società Italiana di Ottica e Fotonica (Italy)

Published by
SPIE—The International Society for Optical Engineering

Volume 6183

The International Society for Optical Engineering